Biochemical and Biophysical Research Communications 417 (2012) 84–87

Contents lists available at SciVerse ScienceDirect

Biochemical and Biophysical Research Communications

journal homepage: www.elsevier.com/locate/ybbrc

Flaviviral helicase: Insights into the mechanism of action of a motor protein

Eloise Mastrangelo, Martino Bolognesi, Mario Milani *

CNR–Istituto di Biofisica, Università degli Studi di Milano, via Celoria 26, 20133 Milano, Italy
Dipartimento di Scienze Biomolecolari e Biotecnologie, Università degli Studi di Milano, via Celoria 26, 20133 Milano, Italy

ARTICLE INFO

Article history:
Received 10 November 2011
Available online 19 November 2011

Keywords:
Flavivirus helicase
Molecular dynamics simulation
Motor protein
ATP binding
RNA remodeling
Protein structural transitions

ABSTRACT

Motor proteins are involved in crucial cell activities, such as cargo transport or nucleic acid remodeling, by converting the free energy of ATP hydrolysis into motion or mechanical work. Flavivirus helicase is a motor protein involved in dsRNA separation during viral replication, thus essential for virus infection. Since a clear vision of the protein activity, in particular of the relationship between ATP cycling and dynamics, is missing, we carried over a molecular dynamics study on Dengue virus helicase in its ATP bound and unbound states. Our simulations show different opening levels of the ssRNA access site to the helicase core. Specifically, we show that ATP induces a closed state into the ssRNA access site, likely involved in the helicase unwinding activity.

1. Introduction

Flaviviral helicase (F-Hel) comprises the C-terminal portion (about 450 amino acids) of the viral multi-functional non-structural protein 3 (NS3). F-Hel belongs to the helicase superfamily 2 (SF2), which collects enzymes displaying a wide range of functions in DNA and RNA metabolism, including single strand translocations, strand annealing, and protein displacement from nucleotides [1]. Within SF2, F-Hel belongs to the subfamily known as DExH (after the amino acid sequence of the conserved helicase motif II, also known as Walker B motif), and is involved in the separation of template and daughter RNA during viral replication. F-Hel is composed of tree domains (I–III), each spanning about 140–160 residues. The first two domains display a characteristic 'RecA-like' fold [2], composed of a β-sheet hosting six parallel β-strands (topology 1–6–5–2–4–3) surrounded by five α-helices; moreover, domain II contains a β-hairpin protruding toward domain III (located between β-strands 5 and 6). The third domain is mainly built by six antiparallel α-helices. The overall F-Hel structure resembles that of an equilateral triangle, where each domain is placed at a vertex. The center of the triangle, where the three domains converge, contains an evident cleft that was first hypothesized [3], and then observed, to host ssRNA during protein activity [4]. The ssRNA access site in the cleft is located between α-helix 2 of domain II, the β-hairpin protruding from domain II toward domain III, and the C-terminal α-helix 6 of domain III; being surrounded by two α-helices, we will refer to the ssRNA access site as the "α-helical gate".

Helicases are able to convert the free energy of ATP hydrolysis into mechanical strain that is used to walk directionally along ssRNA and unwind dsRNA. Different mechanistic models describe the unwinding process as "active" (the protein induces double strand melting) or "passive" (the protein takes advantage of thermal fluctuation causing ds opening and progresses along ssRNA) [5]. For F-Hel, we previously proposed that part of the protein mechanical action on dsRNA could result from a "scissor-like" structural rearrangement, involving mainly domains II and III, occurring near the ssRNA access into the protein cleft [3]. Such conformational rearrangement of F-Hel, suggested by normal mode analysis, essentially describes "open" and "closed" states of the α-helical gate.

Crystallographic investigations have recently disclosed several structural features of the interaction between SF2 Hels belonging to DExH subfamily and ssRNA, in the presence/absence of different ATP analogs. High resolution results have been reported for Dengue virus Hel (DV-Hel) [4] and Hepatitis C virus Hel (HCV-Hel [6–8]). In particular, the recent publication on HCV-Hel [8] has unraveled the protein structural changes induced by ATP analogs mimicking the transition state occurring during ATP hydrolysis. Other theoretical approaches based on elastic networks provided complementary insight into the large structure fluctuations associated to protein activity [9,10]. Although belonging to the same Hel subfamily, F- and HCV-Hel are dissimilar in many features including: (i) different activities on DNA and RNA, (ii) quaternary assembly during function, (iii) important differences mainly in the structure of the domain III and in critical amino acids, e.g. Trp501 (in HCV, [6]) controlling the exit of ssRNA from the protein.

* Corresponding author at: CNR–Istituto di Biofisica, Università degli Studi di Milano, via Celoria 26, 20133 Milano, Italy. Fax: +39 02 50314895.
E-mail address: mario.milani@unimi.it (M. Milani).

0006-291X/$ - see front matter © 2011 Elsevier Inc. All rights reserved.
doi:10.1016/j.bbrc.2011.11.060

Despite the experimental results collected so far, a clear vision of the protein mechanism of action appears still missing. In particular, the different structural states of F-Hel that must be induced by ATP/ADP/apo cycling have not be completely addressed.

In this work we used molecular dynamics simulation (MD) to focus our attention on the structural changes occurring in F-Hel in presence/absence of ATP. In particular, we show that in the absence of RNA substrate and without ATP, DV-Hel displays both open and closed conformations of the α-helical gate. During the simulation time (~41 ns) the protein displays transition from open to closed conformations of the α-helical gate, spending most of the time in a intermediate state. On the contrary, the binding of ATP forces DV-Hel to maintain the 'closed' state along the whole simulation time. We show that such behavior is due to the concerted action of few residues and selected secondary structure elements, which together build up a molecular "transmission shaft", connecting the ATP site (signal site) to the dsRNA access site (effector site).

2. Materials and methods

2.1. Apo protein

The molecular dynamics (MD) simulations started from the atomic coordinates of F-Hel from Dengue virus serotype 4 (451 amino acids; PDB ID: 2JLQ, [4]). Using the program *psfgen* (part of the namd2 package, [11]) H-atoms were added and partial charges assigned to every atom in the structure. Then a box was built around the protein ($71.3 \times 77.2 \times 70.2$ Å^3) and filled with 9247 molecules of water. The charge equilibration of the system was performed adding KCl 0.5 M (43 Cl^- and K^+ ions, using the vmd package; http://www.ks.uiuc.edu/Research/vmd/). Initially, harmonic constraints to fix protein atom positions during energy minimization of the solvent was applied for 0.5 ns, and then the system was equilibrated at 310 K for additional 0.5 ns. Afterward, the simulation was started and lasted ~41 ns, with 2 fs time step (namd2 package, [11]). In particular, the simulation used periodic boundary conditions in NPT ensemble, with Langevin temperature control (T = 310 K) and Langevin piston Nose–Hoover method [12], to maintain constant temperature and pressure, respectively. During the simulation, van der Waals interactions were handled with a cutoff of 12 Å, and switched off using a smoothing function beyond 10 Å. The electrostatic interactions were treated with the Particle Mesh Ewald method [13], using a grid of 100 points along each dimension of the simulation box.

2.2. ATP bound protein

To model the ATP bound DV-Hel we used the atomic coordinates of the apo-protein (PDB ID: 2JLQ) and the structure of the AMPPNP bound protein (PDB ID: 2JLR). The latter was used to model ATP, Mg^{2+} as well as the conformations of the amino acids around the ATP binding site (amino acids from 184 to 208). As a result, the starting model produced to simulate protein dynamics in the presence of ATP was identical to the apo-protein model except for the addition of the ligands (ATP and Mg^{+2}) and the different conformations of 24 amino acids (5.3% of the protein). The model was enclosed in a box ($71.3 \times 77.2 \times 70.2$ Å^3) filled with 9167 water molecules. The charge equilibration was performed adding KCl 0.5 M (42 Cl^- and 44 K^+ ions; using the vmd package; http://www.ks.uiuc.edu/Research/vmd/). The same procedure described for the apo-protein was used to minimize and equilibrate the model, maintaining the same simulation parameters in order to retain the same systematic errors in the two cases.

3. Results

To explore the dynamic changes induced by ATP binding we used all atoms MD simulations run on DV-Hel in the absence and in presence of ATP. In order to avoid spurious behavior generated by different starting coordinates we chose to initiate both the simulations (in presence/absence of ATP) using the crystal structure of DV-Hel apo-protein (PDB ID: 2JLQ), except for some minor changes modeled around the ATP site when the ligand was present (see Section 2); both simulations lasted about 41 ns.

It is possible to summarize the overall MD simulation run using principal component analysis [14]. Briefly, the covariance matrix of protein coordinates during the simulation can be diagonalized, with the highest eigenvalues representing the larger positional fluctuations, and the corresponding eigenvectors representing the main collective motions within the protein. In our simulation, the covariance matrix of Cαs in the absence of ATP shows a large anticorrelated motion involving domain II (amino acids 160–240) and III (360–451) indicating a scissor like swinging of the two domains, as already observed in normal mode analysis [3]. On the contrary, such low frequency structural rearrangement almost vanishes in the presence of ATP, as demonstrated also by the difference between the sum of the two principal covariance eigenvalues in the presence and in the absence of ATP, varying from 3.1 to 5.1 (arbitrary units), respectively.

Moving from domain rearrangements to fine molecular details, we analyzed the differences in the opening state of the dsRNA access site, using as reference parameter the distance between the Cα atoms of Ile365 and Asp603, located at the edges of helix 2 (domain II) and helix 6 (the last helix in domain III), respectively. During the simulation of the apo-protein both open and closed states are occupied without any significant change in protein energy. In particular, the α-helical gate is open (9.8 Å) for the first 6 ns, then closed (6.5 Å) until ~15 ns, and finally maintains an intermediate opening state (7.8 Å), with short transitions toward both open and closed conformations, as reported in Fig. 1. On the contrary, the presence of ATP shifts the dynamical equilibrium of the α-helical gate toward the closed state (6.2 Å), which is constantly occupied without transitions until the end of the simulation (43.5 ns; Fig. 1). Thus, the MD simulations suggest that ATP affects markedly the natural swinging of the protein structure, regulating the dynamical behavior of the α-helical gate located at 30 Å from the ATP binding site.

The intramolecular signal transmission between the ATP site and the α-helical gate depends on the key role of few amino acids and of selected secondary structure elements. In particular, in the presence of ATP, Asn416 (in Hel motif V) is pulled toward the nucleotide, and exchanges a hydrogen bond with an O atom of the α-phosphate during 78% of the simulation (donor–acceptor distance/angle cutoff 3.3 Å/30°). The conserved residue Gly414 is H-bonded to the Mg^{2+}-bound Glu285 (100%), promoting structural stabilization of the preceding residues (Asp409–Glu412) into a 3_{10} helix, only partially present in the apo structure (less than 30% of the simulation time). Interestingly, the amino acids of the mentioned 3_{10} helix are disordered in some F-Hels apo crystal structures (i.e. Japanese Encephalitis Virus; PDB ID: 2Z83) and are subjected to structural transitions in HCV Hel after binding of ATP analogous [8]. The 3_{10} helix (Asp409–Glu412), whose axis runs perpendicularly to the ATP binding site, transfers the displacement of Asn416 and Gly414 toward the ssRNA entrance site (Fig. 2). Since the 3_{10} helix is linked to β-strand 4 in domain II, the latter changes the direction of displacement (from horizontal to vertical as in Fig. 2) and, involving the whole β-sheet of domain II, amplifies the structural rearrangement.

Such wave of structural changes and in particular the shift of motif V toward ATP is locked by a tripartite salt bridge involving

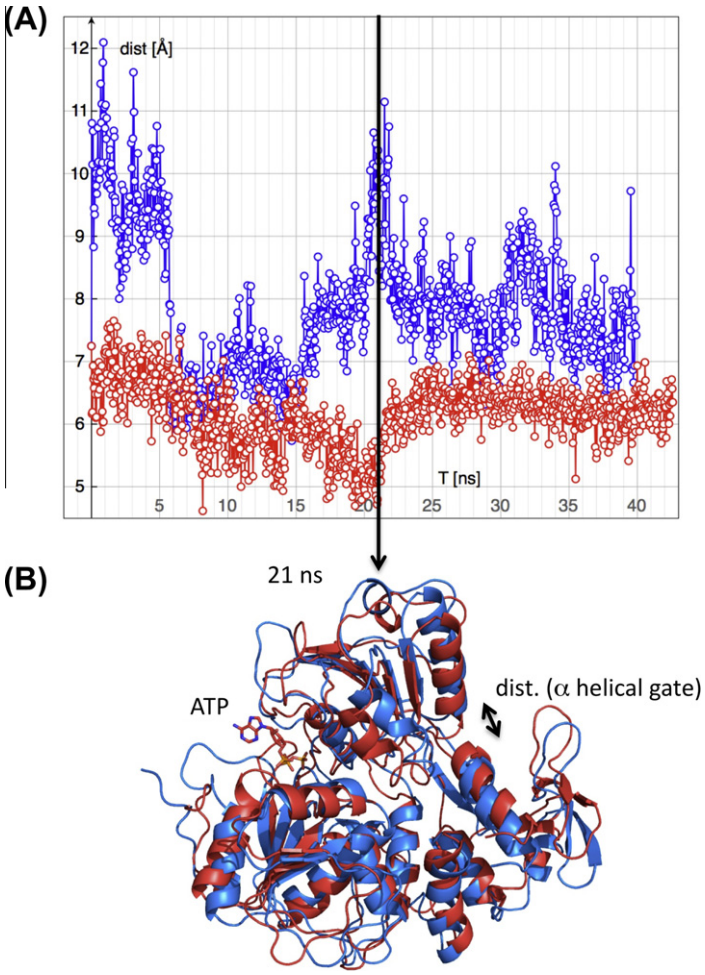

Fig. 1. MD simulation of DV-Hel in the absence/presence of ATP. (A) A plot of the time evolution of the distance between Ile365 and Asp603 (lining the α-helical gate) Cα atoms during the simulation, in the presence (red) and in the absence (blue) of ATP. (B) Superposition of two DV-Hel structures in the presence (red) and in the absence (blue) of ATP, after ~21 ns of MD. Figures created using PyMol (http://www.pymol.org). (For interpretation of the references to color in this figure legend, the reader is referred to the web version of this article.)

Asp409 (again in motif V), Arg387 (at the C-terminal end of β-strand 3 in domain II) and Asp290 (domain I), whose occupancy change from 0.2% to 83% in the presence of ATP To summarize, the horizontal pulling of motif V (Gly414, Asn416, helix 3_{10}) toward ATP (Fig. 2) is amplified and transformed in vertical displacement by the β-sheet of domain II, resulting in the closure of α-helix 2 in domain II (ssRNA access site; Fig. 2). The closure of the other helix lining the ssRNA access site (α-helix 6 in domain III) is likely caused by hydrogen bonds/salt bridges between Asp609 (α-helix 6) and Lys388 (C-terminal end of β-strand 3 in domain II) (occupancy from 28% to 51% in presence of ATP) and Ser386/Asp603 (from 6% to 50%).

4. Discussion

F-Hels belong to the class of motor proteins: they can exploit ATP hydrolysis to convert chemical energy into mechanical work. We are interested in the mechanism of action of this molecular machine and specifically in intramolecular signal transmission from the ATP binding site to the protein active site, where dsRNA unwinding occurs. We should keep in mind that is not possible to exactly localize the Hel active site, since RNA unwinding must involve the concerted action of a wide region of the protein. Such region both triggers Hel progression along ssRNA and, presumably, destabilizes the ss/dsRNA fork (in case of active Hel mechanism [15]), thus inducing dsRNA separation. On the other hand, it is known that the dsRNA access site to the protein is located between α-helix 2 of domain II, the β-hairpin protruding from domain II, and α-helix 6 of domain III; such site is at about 30 Å from the ATP binding site. The idea that drove our work was that ATP binding/ADP releasing cycles must induce recurring structural transitions on the protein, resulting in RNA remodeling. Therefore, the first question to be posed for a deeper understanding of the Hel action is related to the differences in structure/dynamics between the ATP-bound and the apo-protein.

The available experimental evidences based on protein crystal structures [4] show only two different structural states of F-Hel that appear not to depend on the ligation state of the ATP binding site, but only on the presence/absence of ssRNA. In fact, if we take as reference the apo structure (PDB ID: 2JLQ) the r.m.s.d. values calculated superposing on it the AMPPNP- (PDB ID: 2JLR) and ADP-bound (PDB ID: 2JLR) structures are 0.88 and 0.66 Å, respectively (considering 432 Cα pairs). On the other hand, for the remaining six structures (all with RNA bound and different states of the ATP binding site) the r.m.s.d. values relative to the apo structure are considerably higher (the average value is 1.84 + 0.05 Å; on 420 Cαs). Finally, the six structures with RNA bound are quite similar, showing r.m.s.d. values in the range of 0.44 + 0.05 Å (considering 450 Cα pairs. These observations demonstrate that it is possible to divide the nine structures [4] into two structural ensembles: one

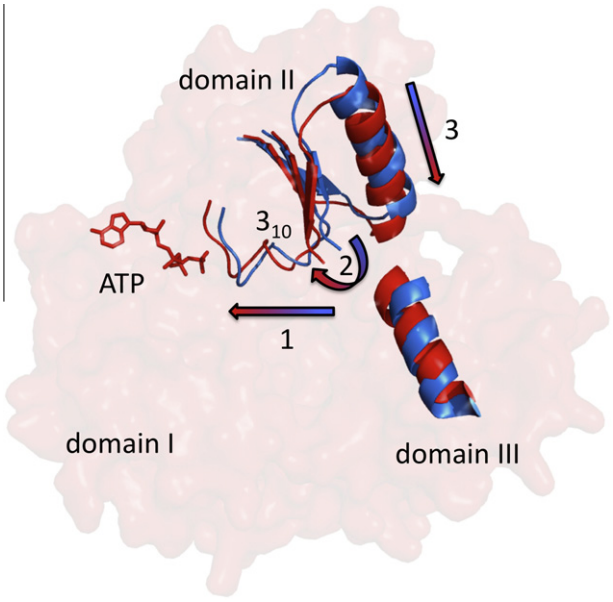

Fig. 2. ATP binding causes the closure of α-helical gate. Superposition of two structures after ~2 ns of MD. The highlighted structural elements (red with ATP, and blue without ATP) indicate the structural changes induced by ATP: (1) motif V (including 3_{10} helix) is pulled toward ATP; (2) pulling is transmitted to the β-sheet of domain II that causes a change in its direction (from horizontal to vertical); (3) β-sheet displacement causes the closure of helix 2 in domain II. (For interpretation of the references to color in this figure legend, the reader is referred to the web version of this article.)

grouping the three structures without RNA, and the other containing the remaining six structures with RNA bound, ignoring both the presence and the kind of ligand in ATP binding site. Consequently, the nine structures reported by Luo et al. even though providing a precious amount of high resolution details, still conceal the dynamics of the system and in particular the relationship between ATP cycling and protein motion. On the contrary, our simulations highlight a clear structural transition that depends on the protein interaction with ATP, and propagates from the ATP binding site to the α-helical gate, thus toward the protein active site. The time-progress of such structural transition can be summarized in a cyclic process whereby: (1) The F-Hel bound ATP induces a closed conformation of the dsRNA access site; (2) ATP is hydrolyzed to ADP that loses affinity for the protein and leaves the binding site; (3) the apo-protein fluctuates between open and closed states, likely promoting dsRNA melting.

Since the 3_{10} helix of motif V (induced by ATP binding) is in contact with ssRNA along its phosphate chain [4], we can speculate that the horizontal oscillations observed for motif V in presence/absence of ATP (Fig. 2) might be one of the main components of the driving force pulling the protein along ssRNA. Moving forward our speculation, we can imagine that the melting of helix 3_{10} (in the absence of ATP) can promote the shift of its amino acids toward 5′ end of the bound ssRNA chain, and that 3_{10} helix reconstitution after ATP binding can partly pull the ssRNA chain in the direction of its 3′ end.

Acknowledgment

This work was funded by the FP7 HEALTH-2010 Collaborative Project SILVER (No. 260644).

References

[1] A.M. Pyle, Translocation and unwinding mechanisms of RNA and DNA helicases, Annual Reviews of Biophysics 37 (2008) 317–336.
[2] S.S. Velankar, P. Soultanas, M.S. Dillingham, H.S. Subramanya, D.B. Wigley, Crystal structures of complexes of PcrA DNA helicase with a DNA substrate indicate an inchworm mechanism, Cell 97 (1999) 75–84.
[3] E. Mastrangelo, M. Milani, M. Bollati, B. Selisko, F. Peyrane, V. Pandini, G. Sorrentino, B. Canard, P.V. Konarev, D.I. Svergun, X. de Lamballerie, B. Coutard, A.A. Khromykh, M. Bolognesi, Crystal structure and activity of Kunjin virus NS3 helicase; protease and helicase domain assembly in the full length NS3 protein, Journal of Molecular Biology 372 (2007) 444–455.
[4] D. Luo, T. Xu, R.P. Watson, D. Scherer-Becker, A. Sampath, W. Jahnke, S.S. Yeong, C.H. Wang, S.P. Lim, A. Strongin, S.G. Vasudevan, J. Lescar, Insights into RNA unwinding and ATP hydrolysis by the flavivirus NS3 protein, EMBO Journal 27 (2008) 3209–3219.
[5] M.D. Betterton, F. Julicher, Opening of nucleic-acid double strands by helicases: active versus passive opening, Physical Review E – Statistical Nonlinear, and Soft Matter Physics 71 (2005) 011904.
[6] J.L. Kim, K.A. Morgenstern, J.P. Griffith, M.D. Dwyer, J.A. Thomson, M.A. Murcko, C. Lin, P.R. Caron, Hepatitis C virus NS3 RNA helicase domain with a bound oligonucleotide: the crystal structure provides insights into the mode of unwinding, Structure 6 (1998) 89–100.
[7] S.G. Mackintosh, J.Z. Lu, J.B. Jordan, M.K. Harrison, B. Sikora, S.D. Sharma, C.E. Cameron, K.D. Raney, J. Sakon, Structural and biological identification of residues on the surface of NS3 helicase required for optimal replication of the hepatitis C virus, Journal of Biological Chemistry 281 (2006) 3528–3535.
[8] M. Gu, C.M. Rice, Three conformational snapshots of the hepatitis C virus NS3 helicase reveal a ratchet translocation mechanism, Proceedings of the National Academy of Sciences of the United States of America 107 (2010) 521–528.
[9] H. Flechsig, D. Popp, A.S. Mikhailov, In silico investigation of conformational motions in superfamily 2 helicase proteins, PLoS ONE 6 (2011) e21809.
[10] H. Flechsig, A.S. Mikhailov, Tracing entire operation cycles of molecular motor hepatitis C virus helicase in structurally resolved dynamical simulations, Proceedings of the National Academy of Sciences of the United States of America 107 (2010) 20875–20880.
[11] J.C. Phillips, R. Braun, W. Wang, J. Gumbart, E. Tajkhorshid, E. Villa, C. Chipot, R.D. Skeel, L. Kale, K. Schulten, Scalable molecular dynamics with NAMD, Journal of Computational Chemistry 26 (2005) 1781–1802.
[12] S.E. Feller, Y. Zhang, R.W. Pastor, and B.R. Brooks, Constant pressure molecular dynamics simulation: the Langevin piston method, AIP, 1995.
[13] T. Darden, D. York, and L. Pedersen, Particle Mesh Ewald: an N log(N) method for Ewald sums in large systems, AIP, 1993.
[14] A. Amadei, A.B. Linssen, H.J. Berendsen, Essential dynamics of proteins, Proteins 17 (1993) 412–425.
[15] M. Manosas, X.G. Xi, D. Bensimon, V. Croquette, Active and passive mechanisms of helicases, Nucleic Acids Research 38 (2010) 5518–5526.